Hao Yang,[1,2] Jiang W. Wu,[2] Shu P. Wang,[2] Ilenia Severi,[3] Loris Sartini,[3] Norma Frizzell,[4] Saverio Cinti,[3] Gongshe Yang,[1] and Grant A. Mitchell[2]

Adipose-Specific Deficiency of Fumarate Hydratase in Mice Protects Against Obesity, Hepatic Steatosis, and Insulin Resistance

Diabetes 2016;65:3396–3409 | DOI: 10.2337/db16-0136

OBESITY STUDIES

Obesity and type 2 diabetes are associated with impaired mitochondrial function in adipose tissue. To study the effects of primary deficiency of mitochondrial energy metabolism in fat, we generated mice with adipose-specific deficiency of fumarate hydratase (FH), an integral Krebs cycle enzyme (AFHKO mice). AFHKO mice have severe ultrastructural abnormalities of mitochondria, ATP depletion in white adipose tissue (WAT) and brown adipose tissue, low WAT mass with small adipocytes, and impaired thermogenesis with large unilocular brown adipocytes. AFHKO mice are strongly protected against obesity, insulin resistance, and fatty liver despite aging and high-fat feeding. AFHKO white adipocytes showed normal lipolysis but low triglyceride synthesis. ATP depletion in normal white adipocytes by mitochondrial toxins also decreased triglyceride synthesis, proportionally to ATP depletion, suggesting that reduced triglyceride synthesis may result nonspecifically from adipocyte energy deficiency. At thermoneutrality, protection from insulin resistance and hepatic steatosis was diminished. Taken together, the results show that under the cold stress of regular animal room conditions, adipocyte-specific FH deficiency in mice causes mitochondrial energy depletion in adipose tissues and protects from obesity, hepatic steatosis, and insulin resistance, suggesting that in cold-stressed animals, mitochondrial function in adipose tissue is a determinant of fat mass and insulin sensitivity.

Human obesity and type 2 diabetes (1–5) and mouse models of obesity, including *ob/ob*, *db/db*, and high-fat fed (6,7), are associated with low mitochondrial function in white adipose tissue (WAT). Whether compromised adipose mitochondrial function is a cause or consequence of obesity and diabetes remains unclear. Mitochondrial function is essential for normal WAT and brown adipose tissue (BAT). WAT shows low energy consumption (8), but mitochondria are necessary for white adipocyte function (9). The principal functions of WAT are triglyceride (TG) synthesis, which requires energy, and release of fatty acids in response to energy demand, which does not consume energy. In contrast, BAT is mitochondria rich, performing nonshivering thermogenesis by uncoupling oxidative phosphorylation (OXPHOS) (10,11), which requires intense mitochondrial energy production.

Few studies have examined primary mitochondrial dysfunction in adipocytes. Mice with adipose-specific deficiencies of mitochondrial DNA translation factor Crif1 (CR6-interacting factor 1) and mitochondrial transcription factor A (TFAM) were created by Cre-lox–mediated gene excision. aP2-Cre–mediated gene excision occurs in macrophages (12) and other cells (13) as well as in adipocytes. aP2-Crif1$^{-/-}$ mice show low weight gain and poor development of adipose tissues and die within 24 days of birth. White and brown aP2-Crif1$^{-/-}$ adipocytes contain swollen mitochondria with distorted cristae. Heterozygous aP2-Crif1$^{+/-}$ mice have insulin resistance,

[1]Laboratory of Animal Fat Deposition and Muscle Development, College of Animal Science and Technology, Northwest A&F University, Yangling, Shaanxi, China
[2]Division of Medical Genetics, Department of Pediatrics, Université de Montréal and CHU Sainte-Justine, Montreal, Quebec, Canada
[3]Department of Experimental and Clinical Medicine, Center of Obesity, United Hospitals, University of Ancona (Università Politecnica Delle Marche), Ancona, Italy
[4]Department of Pharmacology, Physiology & Neuroscience, School of Medicine, University of South Carolina, Columbia, SC

Corresponding author: Grant A. Mitchell, grant.mitchell@recherche-ste-justine.qc.ca, or Gongshe Yang, gsyang999@hotmail.com.

Received 28 January 2016 and accepted 16 August 2016.

This article contains Supplementary Data online at http://diabetes.diabetesjournals.org/lookup/suppl/doi:10.2337/db16-0136/-/DC1.

macrophage infiltration in WAT, and systemic inflammation (14). aP2-TFAM$^{-/-}$ mice have low mitochondrial DNA (mtDNA) and protein contents, high energy expenditure, leanness, and insulin sensitivity (15). Adipoq-Cre–mediated gene excision occurs exclusively in adipocytes (16). Adipoq-TFAM$^{-/-}$ mice show lipodystrophy, insulin resistance, hepatic steatosis, and WAT inflammation (17).

Adipose-specific deficiency of an essential mitochondrial enzyme has not been studied. Fumarate hydratase (FH; E.C. 4.2.1.2), an integral Krebs cycle enzyme, catalyzes the reversible hydration of fumarate to malate. Mitochondrial and cytosolic isoforms of FH are transcribed from different promoters of the *FH* gene (18). Cytosolic FH acts in the urea cycle (19), principally in liver and kidney (20) but not in adipose tissue. Two intriguing clinical forms of FH deficiency are known in humans. Autosomal recessive partial systemic FH deficiency (Online Mendelian Inheritance in Man 136850) causes severe encephalopathy, massive fumarate excretion, and often death in infancy (21,22). The autosomal dominant syndrome, hereditary cutaneous and uterine leiomyomas and renal cell cancer (Online Mendelian Inheritance in Man 605839), occurs in heterozygotes for null *FH* mutations wherein cells with somatic loss of the normal *FH* allele may develop into tumors (23,24). Complete systemic FH deficiency is lethal in mouse embryos (25) and is not reported in humans; thus, we generated adipose-specific Adipoq-Cre–mediated FH knockout (AFHKO) mice.

RESEARCH DESIGN AND METHODS

Generation and Rearing of AFHKO Mice

A conditional FH targeting vector was constructed by inserting LoxP sites flanking FH exon 3 (Supplementary Fig. 1). Gene targeting was performed in 129Sv/J-derived J1 mouse embryonic stem cells (26). Positive embryonic stem cell clones, confirmed by Southern blotting, were used to generate chimeras. After germline transmission, these were backcrossed to a C57BL/6J background for more than eight generations and then bred to B6;FVB-Tg(Adipoq-cre)1Evdr/J mice (The Jackson Laboratory, Bar Harbor, ME) to produce FH flox/flox Cre+ mice, henceforth designated AFHKO. FH flox/flox Cre− mice were used as controls. PCR-based genotyping was performed to distinguish among normal (+/+), homozygous-targeted (lox/lox), and heterozygous (+/lox) mice. Three primers were used to amplify mouse tail DNA: Mfum12, Mfum26, and Neo-1 (Supplementary Table 1). Mice were reared at 21°C in a 12-h dark/light cycle with free access to water and regular chow (2019 Teklad Global; Harlan Laboratories) or high-fat chow (F3282; Bio-Serv). Experiments were approved by the Canadian Council on Animal Care–certified animal facility committee of CHU Sainte-Justine.

Real-Time PCR Assessment of Transcript and mtDNA Levels

This was performed as previously described (27). mtDNA content was measured by using 200 ng of total DNA purified from adipose tissue. Amplification of the mitochondrial *12S rRNA* gene was compared with that of reference nuclear gene *GCG*. Supplementary Table 2 shows the primers.

Western Blotting

Western blotting was performed as previously described (27). Antibodies were antifumarase (4567S; Cell Signaling Technology [CST]), anti-uncoupled protein 1 (UCP1) (RB-10599-P0; Neomarkers), antiperilipin A (P1998; Sigma), anti-acetyl-CoA carboxylase (ACC) (3676P, CST), anti-ATP citrate lyase (ACLY) (4332P; CST), anti-fatty acid synthase (FAS) (sc-20140; Santa Cruz Biotechnology), anti-GAPDH (5174P; CST), anti-Akt (9272S; CST), and antiphospho-Akt (Ser473) (9271S; CST). Succination of adiponectin was detected as previously described (28).

Fumarate and Succinate Measurement

Fumarate (K633-100; BioVision) and succinate (ab204718; Abcam) contents were determined colorimetrically by following manufacturers' instructions.

Enzyme Activity Assay

Citrate synthase (CS) and FH were assayed as previously described (29,30).

Mitochondrial Isolation and Blue Native PAGE

Mitochondria from isolated perigonadal white adipocytes and from interscapular brown adipocytes were prepared as previously described (15), and then OXPHOS complexes were resolved on a 4–20% nondenaturing PAGE gradient (4561094; Bio-Rad). After transfer to a polyvinylidene fluoride membrane, incubation was performed with the following anti-OXPHOS antibodies from Abcam: anti-NDUFA9 (complex I, ab14713), anti-SDHA (complex II, ab14715), anti-ubiquinol-cytochrome c reductase core protein I (complex III, ab110252), anti-COX4 + COX4L2 (complex IV, ab110261), and anti-ATP5A (complex V, ab14748).

ATP Measurement

ATP content was assayed by luminometry (A22066; Invitrogen) by following the manufacturer's instructions. Briefly, frozen adipose tissues were homogenized in 200 μL cold sterile H_2O and then centrifuged at 12,000*g* for 10 min at 4°C. Ten microliters of supernatant were mixed with 90 μL of reaction solution and shielded from light. Luminance was measured 10 min later.

Microscopy and Morphometry

Histological analysis of adipose tissues was as previously described (27). For transmission electron microscopy, mice were perfused transcardially with 50 mL of 2% glutaraldehyde in 0.1 mol/L phosphate buffer (pH 7.4), and adipose tissues were prepared as previously described (31).

Body Composition

Lean and fat masses were evaluated by DEXA scanning as previously described (32).

TG Synthesis

TG synthesis in isolated adipocytes was measured as previously described (33), except that the reaction volume was 0.5 mL rather than 3 mL.

Acute β3-Adrenergic Stimulation In Vivo

This was performed as previously described (32). Mice were fasted 5 h before testing. The β3-adrenergic receptor–specific agonist CL 316,243 (C5976; Sigma-Aldrich) was used.

Body Temperature Measurement

Rectal temperature was monitored with a BAT-10 Thermometer (Physitemp Instruments, Clifton, NJ).

Insulin Tolerance and Glucose Tolerance Testing

These were performed as previously described (27), starting with the insulin tolerance test (ITT) and then the glucose tolerance test (GTT) 10 days later.

Plasma Metabolites, Tissue TG, and Fecal Lipid Content

Plasma insulin, leptin, TG, nonesterified fatty acid (NEFA), and adiponectin were assayed with commercial kits (27), and total tissue TG and fecal lipids were assayed as previously described (32,34).

Food Consumption

Mice were housed individually. Food was weighed twice daily for 1 week at 9:00 A.M. and 5:00 P.M.. The interval between 9:00 A.M. and 5:00 P.M. was designated as day consumption and that between 5:00 P.M. and 9:00 A.M. the next day was designated as night consumption.

Calorimetry

After acclimatization in metabolic chambers for 48 h, mice were assessed for 48 h, with free access to food and water throughout. VO_2, VCO_2, energy expenditure, and physical activity were measured as previously described (32) with an Oxymax/Comprehensive Lab Animal Monitoring System (Columbus Instruments, Columbus, OH). VO_2, VCO_2, and energy expenditure data were adjusted to lean body mass.

Thermoneutrality

Eight pairs of 9-month-old AFHKO and control mice were housed at 30°C for 1 month. Food consumption was measured, and ITT, GTT, and DEXA scanning were performed at 21°C (before) and at 30°C (after 1 month at thermoneutrality).

Statistical Analysis

Data are presented as mean ± SEM. Groups were compared by the paired two-tailed Student *t* test.

RESULTS

FH Is Inactivated in WAT and BAT of AFHKO Mice

AFHKO mice were born in the expected Mendelian ratio and were viable. FH mRNA expression in AFHKO WAT and BAT was <9% of control levels (Fig. 1*A*). Because adipose tissues contain nonadipocyte cells, in which FH expression is expected to be normal in AFHKO mice, we assessed FH in isolated adipocyte mitochondria; FH was undetectable (Fig. 1*B*). In other organs of AFHKO mice, FH levels were normal (Fig. 1*C*), confirming adipose-specific gene excision. In AFHKO WAT and BAT, fumarase activity was reduced by 85.5% and 73.4%, respectively, compared with normal controls (Fig. 1*D*). Tissue fumarate (Fig. 1*E*) and plasma fumarate levels (Fig. 1*F*) were higher in AFHKO mice than in controls; tissue succinate levels were similar to control levels (Supplementary Fig. 2). Together, these data show that Adipoq-Cre–mediated FH gene excision in AFHKO mice is complete and adipocyte specific.

FH Deficiency Causes Severe Mitochondrial Dysfunction in WAT and BAT

The ultrastructure of perigonadal WAT from control mice showed normal mitochondria with sparse cristae (Fig. 1*G*). AFHKO WAT adipocyte mitochondria typically were swollen with reduced or absent cristae. Some AFHKO white adipocytes showed cell death, with cytoplasmic degeneration, lipid extrusion into the interstitium, and tissue macrophages nearby (data not shown). Control BAT showed the expected multilocular lipid droplets in the cytoplasm and abundant laminar cristae in mitochondria (Fig. 1*G*). In contrast, AFHKO brown adipocytes were unilocular. Their mitochondria were irregular, elongated, and sometimes giant and had sparse, randomly oriented cristae. In other cell types within adipose tissues, mitochondria appeared normal (Supplementary Fig. 3).

In 5-month-old AFHKO mice, ATP levels were markedly lower than normal in both WAT and BAT (Fig. 1*I* and *M*). However, multiple other parameters of mitochondrial function were strikingly different between AFHKO WAT and BAT. Respiratory chain complexes (Fig. 1*H*), CS activity (Fig. 1*J* and *N*), mtDNA content (Fig. 1*K* and *O*), and transcripts of Krebs cycle enzymes and respiratory chain complexes (Fig. 1*L* and *P*) were generally high in AFHKO WAT but low in AFHKO BAT.

AFHKO Mice Are Obesity Resistant

AFHKO males (Fig. 2*A*) and females (Fig. 2*B*) raised on normal chow until 10 months of age progressively gained less weight than controls. DEXA scanning revealed that this difference was exclusively due to lower fat mass (Fig. 2*C*). This was confirmed by weighing each individual AFHKO WAT fat depot (Fig. 2*D*). It was associated with smaller adipocyte size (Fig. 2*E* and *F*). Mean adipocyte diameter in 5-month-old AFHKO WAT was 53.4 ± 2.3 μm versus 70.3 ± 3.5 μm in controls ($P < 0.001$) (Fig. 2*G*). In contrast, BAT mass of 5-month-old AFHKO mice exceeded that of controls (Fig. 2*D*). AFHKO brown adipocytes were hypertrophic and monolocular (Fig. 2*E*).

The cardinal features of adipose ATP depletion, leanness, small WAT adipocytes, and unilocular, hypertrophic BAT adipocytes were already present in 9-week-old AFHKO mice, when body mass was not yet significantly different between AFHKO and normal animals (Supplementary Fig. 4*A–D*). Similar findings occurred in 10-month-old AFHKO males (Fig. 2*H*) and in 5- and 10-month-old AFHKO females (Supplementary Fig. 5*A* and *B*).

Distinct and Opposite Expression Profiles Related to Cytoplasmic Energy Metabolism Occur in AFHKO WAT and BAT

AFHKO WAT generally showed high expression of genes related to fatty acid and TG metabolism, whereas low

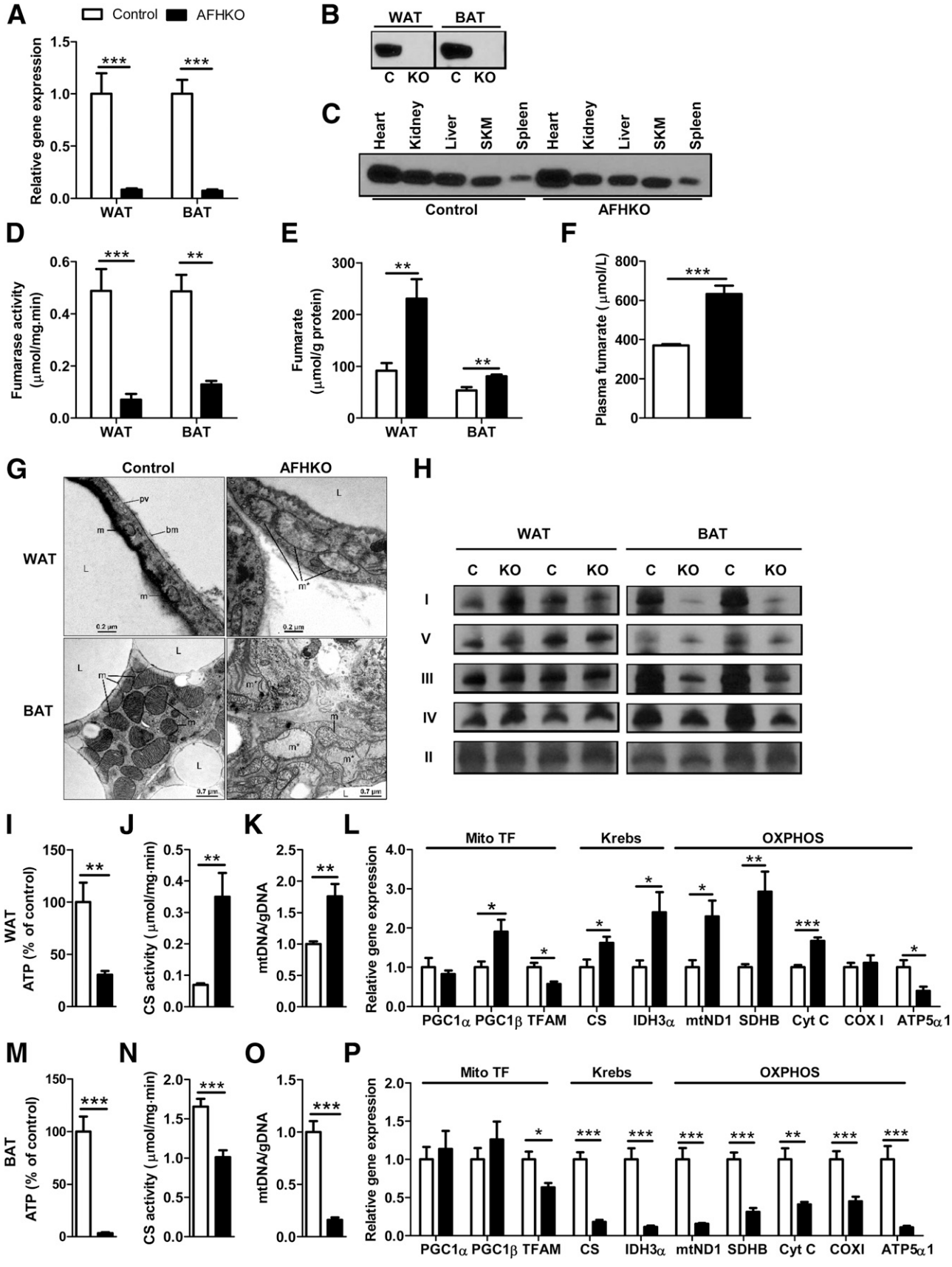

Figure 1—AFHKO mice have adipose-specific FH gene excision. *A*: FH mRNA expression in perigonadal WAT and BAT assayed by real-time PCR ($n = 8$). *B* and *C*: Western blot for FH. Mitochondria were prepared from isolated adipocytes from perigonadal WAT and from BAT of AFHKO and control mice (10 μg mitochondrial protein/lane) (*B*). FH expression in nonadipose tissues (30 μg protein of tissue

levels were seen in AFHKO BAT. In AFHKO WAT, high mRNA expression was observed for genes of glucose uptake (GLUT1 and GLUT4) (Fig. 3*A*); glycolysis (GAPDH and lactate dehydrogenase A [LDHA]) (Fig. 3*B*); lipogenesis, TG synthesis, and related transcription factors (CD36, ACLY, ACC1, FAS, diglyceride acyltransferase 1 [DGAT1], liver X receptor α [LXRα], SREBP1c, and ChREBP) (Fig. 3*C* and *G*); and fatty acid oxidation (carnitine palmitoyltransferase 1β [CPT1β], long chain acyl CoA dehydrogenase [LCAD], and medium chain acyl CoA dehydrogenase [MCAD]) (Fig. 3*H*). In contrast, in AFHKO BAT, expression was not increased for genes of glucose uptake (Fig. 3*D*) and was low for genes of glycolysis, lipogenesis, TG synthesis, and fatty acid oxidation (Fig. 3*E*, *F*, *I*, and *J*). Of note, expression of the key adipose differentiation factor peroxisome proliferator–activated receptor (PPARγ) was unchanged in both AFHKO WAT and BAT (Fig. 3*G* and *I*). Expression levels of key proteins related to lipogenesis were tested by Western blotting. In AFHKO WAT, ACC1, ACLY, and FAS were increased (Fig. 3*K*). In AFHKO BAT, ACC1 was unchanged, but ACLY and FAS were low (Fig. 3*L*). GAPDH was increased in AFHKO WAT (Fig. 3*K*), but in contrast to its low mRNA level in AFHKO BAT (Fig. 3*E*), GAPDH protein was unchanged in AFHKO BAT (Fig. 3*L*).

Reduced Cellular ATP Content Is Associated With Impaired TG Synthesis

We assessed TG synthesis in isolated AFHKO and control adipocytes. TG synthesis was significantly lower in AFHKO adipocytes than in that of controls (Fig. 4*A*). Because of the discordance between expression data in WAT, which predicted a high capacity for TG synthesis, and the previous observations in AFHKO WAT that showed low levels of ATP, small cells, low WAT mass, and low TG synthesis, we explored whether depletion of ATP would reduce TG synthesis in normal white adipocytes. We tested three respiratory chain inhibitors: rotenone (which inhibits complex I), antimycin A (complex III), and oligomycin (complex V). Incubation with each one reduced adipocyte ATP content (Supplementary Fig. 6*A*) and TG synthesis (Supplementary Fig. 6*B*). A strong association was observed between cellular ATP level and TG synthesis (Fig. 4*B*). These data suggest that even in cells with a normal apparatus for TG synthesis, reduction of mitochondrial energy production and depletion of ATP can result in reduced TG synthesis.

AFHKO Mice Show Low Basal Plasma Fatty Acid Levels and Normal Increases Following Lipolytic Stimulation

We evaluated lipolysis in AFHKO mice under three conditions. The plasma NEFA level of AFHKO mice was lower than that of controls after a brief (5-h) fast, consistent with the lower WAT mass of AFHKO mice. After a 48-h fast, however, plasma NEFA levels were similar in AFHKO and control mice (Fig. 4*C*). In addition, acute β3-adrenergic stimulation of lipolysis by injection with the agonist CL 316,243 produced similar increases of plasma NEFA in AFHKO and control mice (Fig. 4*D*). Therefore, in contrast to the deficiency of adipocyte TG synthetic capacity, lipolytic capacity was preserved in AFHKO mice.

Body Temperature Maintenance Is Impaired in AFHKO Mice

AFHKO mice were challenged with cold and fasting. At 21°C, basal body temperature was similar in AFHKO and control mice. However, after 4 h of fasting at 4°C, temperature dropped by 4.5 ± 0.7°C in AFHKO mice (Fig. 4*E*) versus 1.9 ± 0.3°C in controls ($P < 0.01$). At 21°C (Fig. 4*F*), AFHKO mice had similar body temperature to controls 5 h after food removal (37.7 ± 0.2°C vs. 37.2 ± 0.2°C, respectively). After a 48-h fast, the temperature of AFHKO mice was significantly lower (33.9 ± 0.4°C vs. 35.9 ± 0.4°C, respectively, $P < 0.01$).

Compatible with defective adaptive thermogenesis in AFHKO BAT, UCP1 mRNA was only 5.3% of control levels. The β3-adrenergic receptor (ARβ3) transcript was 67% of control levels (Fig. 4*G*), and UCP1 protein was undetectable (Fig. 4*H*). Therefore, AFHKO mice have reduced thermogenic capacity and markedly low levels of UCP1, the key protein of BAT thermogenesis.

AFHKO Mice Are Protected From Age-Related Insulin Resistance

At 3.5 months of age, insulin sensitivity and glucose tolerance were similar in chow diet–fed AFHKO and control mice (Fig. 5*A*). However, at 10 months, control mice had developed some insulin resistance and glucose intolerance, whereas the curves of AFHKO mice were unchanged from their values at 3.5 months (Fig. 5*B*). In addition, compared with normal controls, AFHKO mice had lower plasma levels of insulin, leptin, TG, NEFA, and adiponectin at 5 and 10 months (Fig. 5*C* and *D*).

We studied the phosphorylation of Akt at Ser473 as an indicator of the activity of the insulin signaling pathway

homogenate protein/lane) (*C*). *D* and *E*: FH activity and fumarate content of perigonadal WAT and BAT ($n = 6$). *F*: Plasma fumarate (5-month-old males, $n = 8$). *G*: Representative mitochondrial ultrastructure of perigonadal WAT and BAT from 5-month-old control and AFHKO mice ($n = 5$). *H*: Blue Native PAGE analysis of OXPHOS complexes. Fifteen micrograms of mitochondrial protein were used for WAT and 7.5 μg for BAT ($n = 4$, two representative results shown). *I–L*: Perigonadal WAT: ATP content ($n = 6$) (*I*), CS activity ($n = 6$) (*J*), mtDNA content ($n = 8$) (*K*), and expression levels of genes related to mitochondrial function ($n = 8$) (*L*). *M–P*: BAT as evaluated as in panels *I–L* and in samples from the same mice. $^*P < 0.05$; $^{**}P < 0.01$; $^{***}P < 0.001$. bm, basal membrane; C, control; gDNA, genomic DNA; I, complex I; II, complex II; III, complex III; IV, complex IV; KO, AFHKO; L, lipid droplet; m, mitochondrion; m*, giant mitochondrion; pv, pinocytotic vesicle; SKM, skeletal muscle; TF, transcription factor; V, complex V.

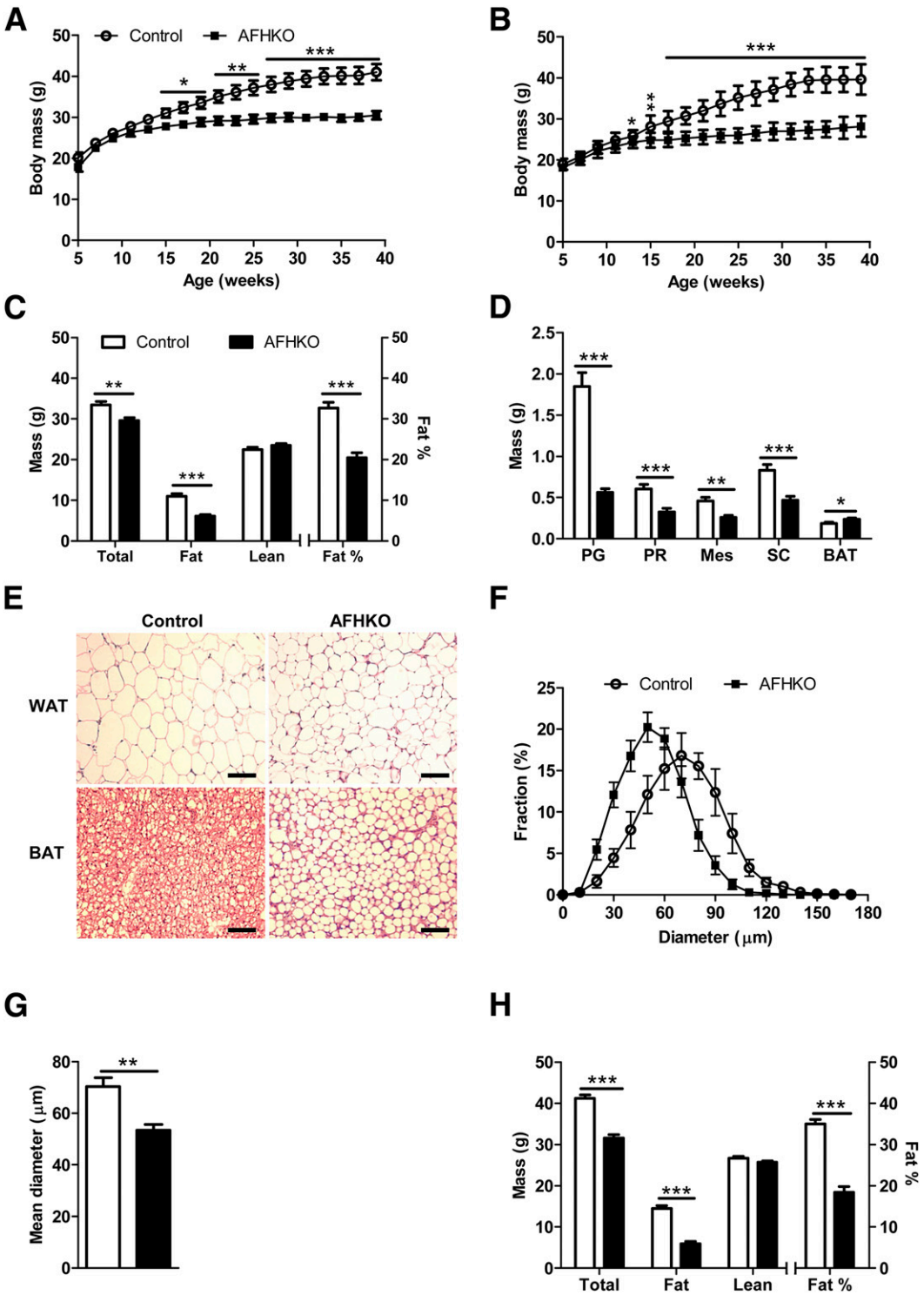

Figure 2—AFHKO mice are protected against aging-induced obesity. *A* and *B*: Growth to 10 months of age in male (*A*) and female (*B*) control and AFHKO mice fed a normal diet (n = 12). *C*: Body composition at 5 months of age (n = 10). Fat percentage refers to fat mass as a fraction of total (lean + fat) mass. *D*: WAT depot masses and BAT mass of control and AFHKO males at 5 months of age. *E*: Representative hematoxylin-eosin–stained sections of WAT and BAT from 5-month-old control and AFHKO mice fed a normal chow diet. Scale bar = 100 μm. *F*: Distribution of white adipocyte diameters in perigonadal WAT (n = 5; ≥315 cells measured/mouse). *G*: Mean adipocyte diameters. *H*: Body composition at 10 months of age (n = 8). $^{*}P < 0.05$; $^{**}P < 0.01$; $^{***}P < 0.001$. BAT, interscapular BAT; Mes, mesenteric; PG, perigonadal; PR, perirenal; SC, subcutaneous.

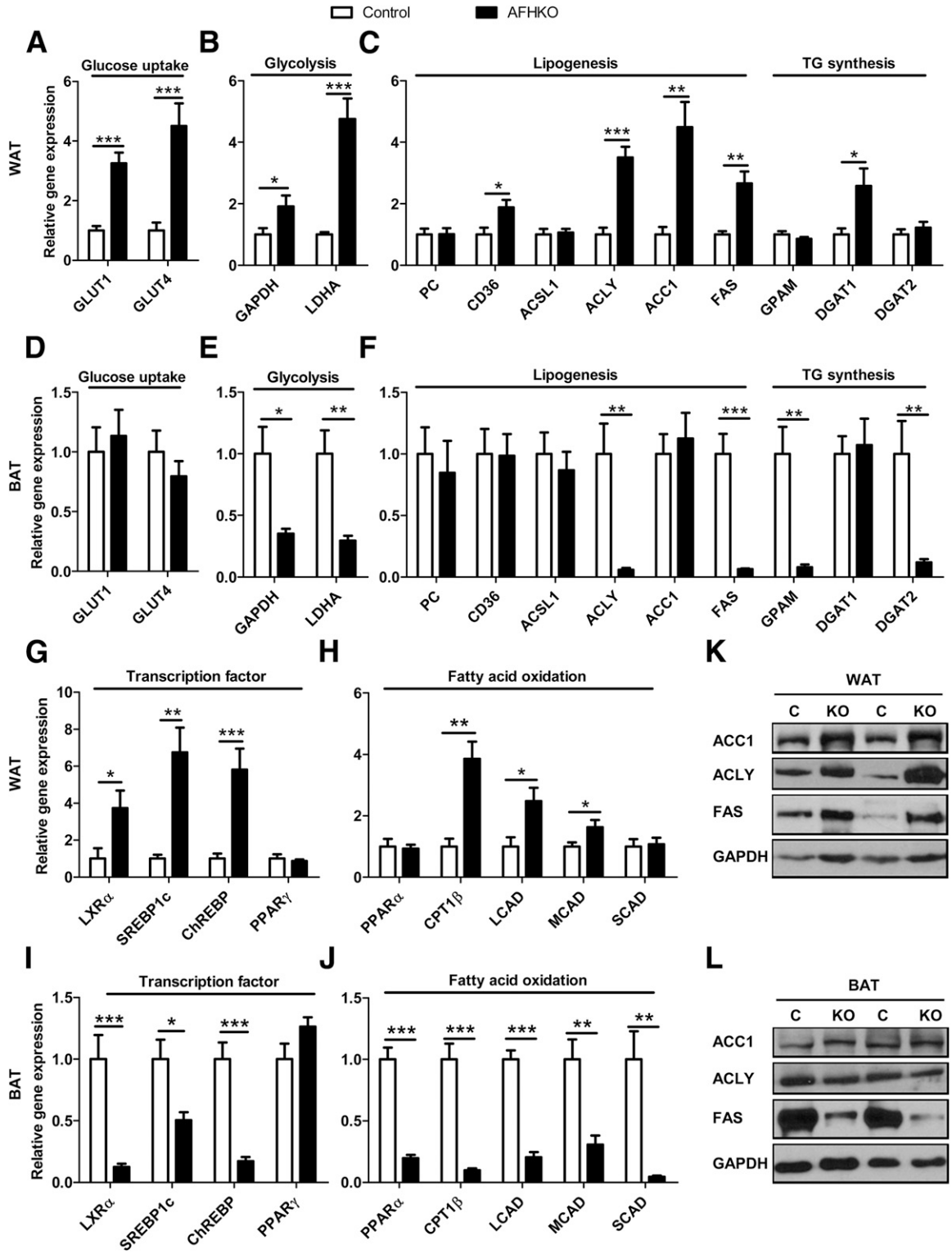

Figure 3—FH deficiency alters gene expression patterns differently in WAT and BAT. *A–C*, *G*, and *H*: Perigonadal WAT. Transcripts related to glucose uptake (*A*), glycolysis (*B*), lipogenesis and TG synthesis (*C*), transcription factors related to lipid energy metabolism (*G*), and mitochondrial fatty acid oxidation (*H*) were measured by real-time PCR. Adipose tissues studied were from 5-month-old male control and AFHKO mice (n = 8). *D–F*, *I*, and *J*: BAT evaluated as described for perigonadal WAT. *K* and *L*: Western blots of the indicated proteins in WAT and BAT, respectively (n = 4, two representative results shown). $^{*}P < 0.05$; $^{**}P < 0.01$; $^{***}P < 0.001$. C, control; KO, AFHKO.

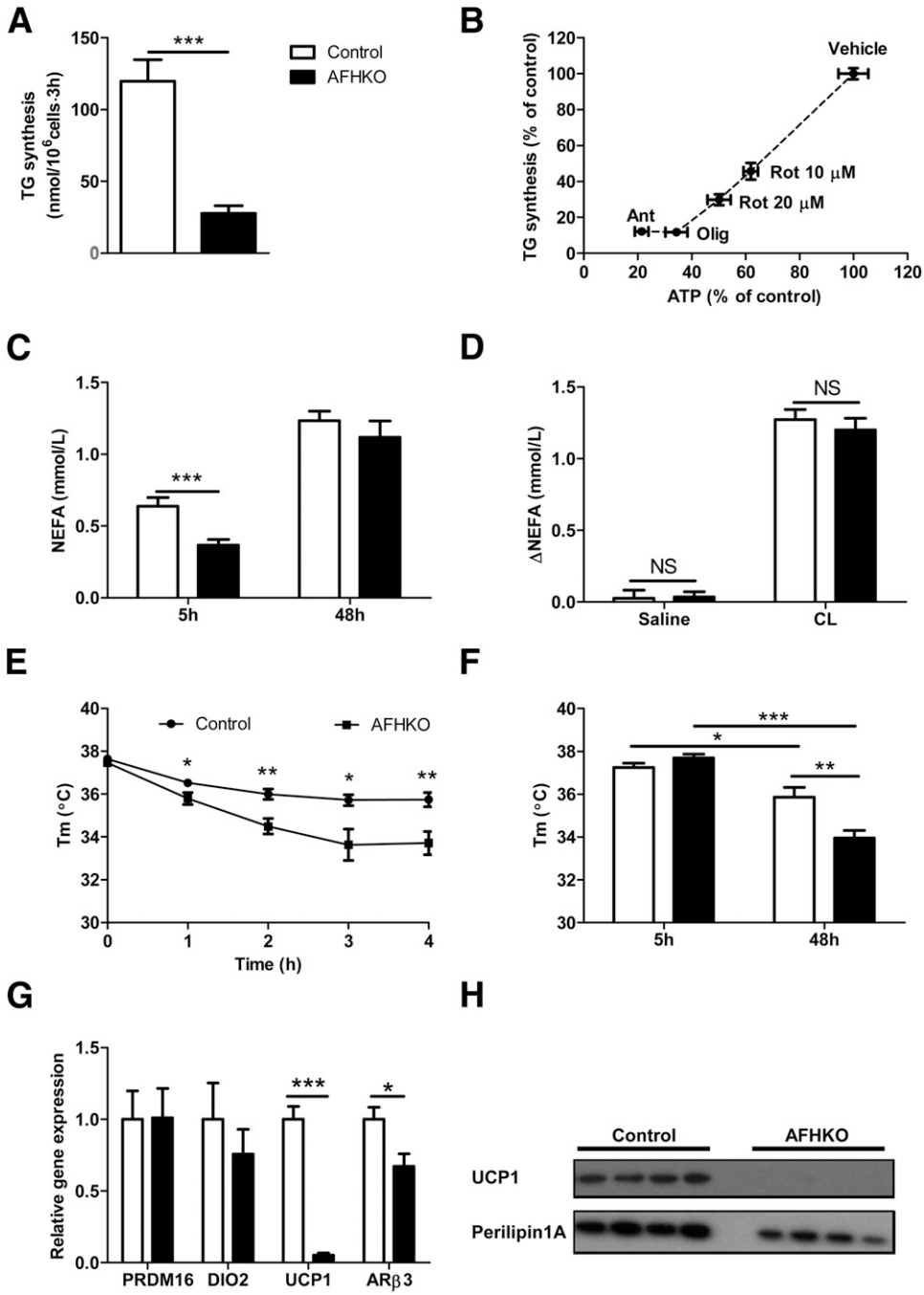

Figure 4—FH deficiency reduces TG synthesis in white adipocytes, allows normal stimulation of lipolysis, and impairs temperature maintenance. *A*: TG synthesis assessed in isolated perigonadal white adipocytes as described in RESEARCH DESIGN AND METHODS (n = 6–7). *B*: Correlation between ATP depletion and reduced TG synthesis (perigonadal adipocytes, 5-month-old mice, n = 6). *C*: Plasma NEFA levels at 5 and 48 h of fasting (5-month-old males, n = 9). *D*: Changes in NEFA levels following injection of saline or β3-adrenergic–specific agonist CL 316,243. Mice were fasted for 5 h and then injected intraperitoneally with saline or CL 316,243 in saline. Tail-vein blood samples were collected before and 15 min after injection for NEFA assay (5-month-old males, n = 12). *E*: Body temperature at 4°C after 4 h of fasting (4-month-old males, n = 12). *F*: Body temperatures at 21°C after 5 and 48 h of fasting (5-month-old males, n = 9). *G*: Thermogenesis-related transcripts in BAT (5-month-old males, n = 8). *H*: UCP1 protein expression in BAT measured by Western blot in control and AFHKO mice (5-month-old males, 30 μg protein/lane). $^*P < 0.05$; $^{**}P < 0.01$; $^{***}P < 0.001$. Ant, antimycin A; CL, CL 316,243; NS, not significant; Olig, oligomycin; Rot, rotenone; Tm, temperature.

in 10-month-old AFHKO mice. In AFHKO WAT, Akt (Ser473) phosphorylation was not different from that of controls (Fig. 5*E* and Supplementary Fig. 7*A*). In AFHKO liver, mean phosphorylation was lower than normal, but this was not significant (Fig. 5*F* and Supplementary Fig. 7*B*). In AFHKO skeletal muscle, phosphorylation was

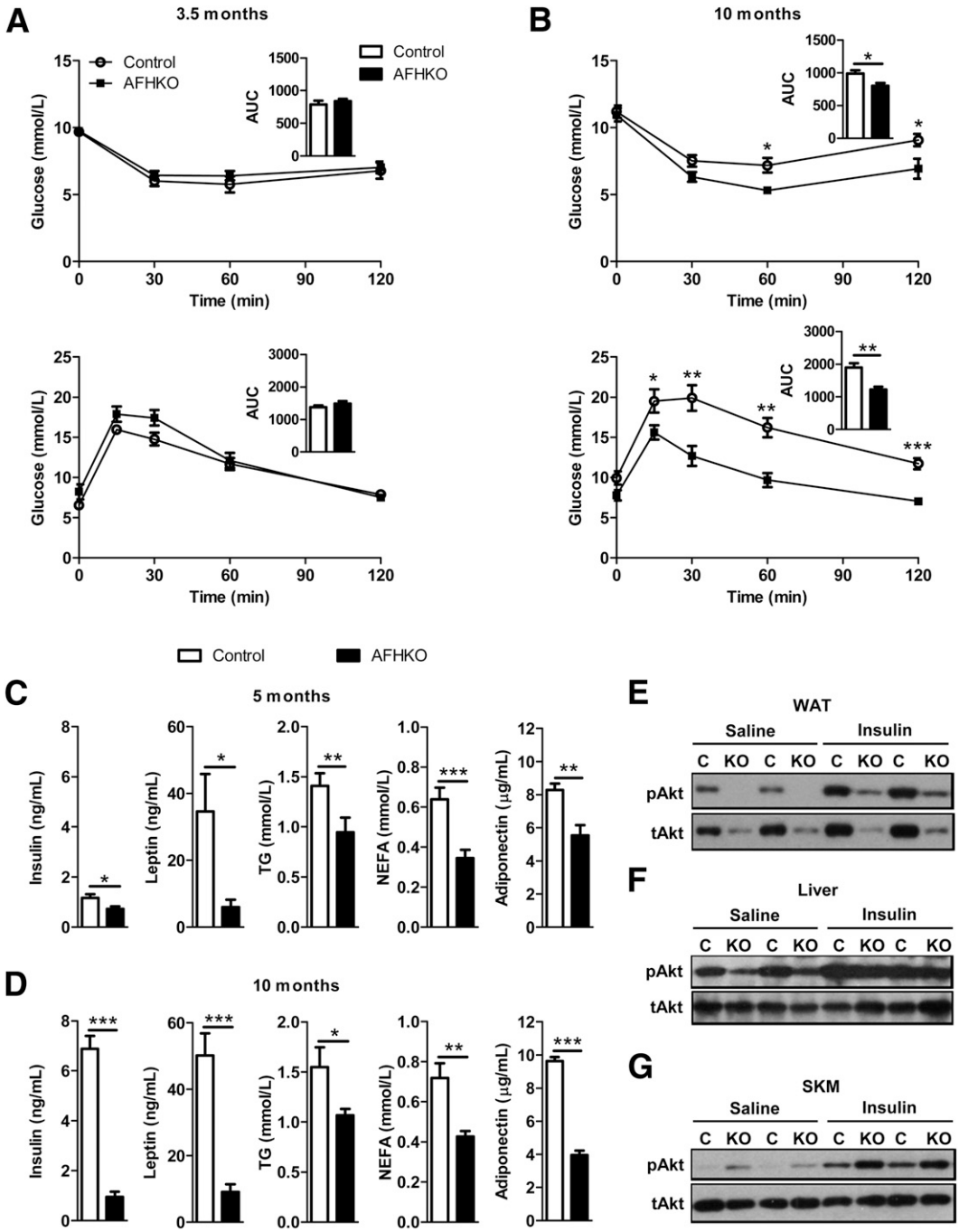

Figure 5—AFHKO mice remain insulin sensitive with aging. *A*: ITT (top) and GTT (bottom) in 3.5-month-old mice. For the ITT, 5 h after food removal at 6:00 A.M., insulin was injected intraperitoneally (1 unit/kg), and blood glucose was measured at the indicated times (n = 8). For the GTT, 14 h after food removal at 6:00 P.M., 1.5 g/kg glucose was injected intraperitoneally (n = 8). *B*: ITT (top) and GTT (bottom) in 10-month-old mice while following the protocols described in panel *A* (n = 6–8). The insets depict areas under the curve (AUCs) in mmol/L · min. *C* and *D*: Plasma levels of insulin, leptin, TG, NEFA, and adiponectin were measured in 5- and 10-month-old mice fasted for 5 h (n = 7–11). *E*–*G*: Western blots of tissue extracts from WAT, liver, and quadriceps skeletal muscle (SKM) 15 min after injection of insulin or saline (4-h fasting and 1 unit/kg insulin injection) probed with antibodies for phospho-Akt (Ser 473) (pAkt) or total Akt (tAkt) (10-month-old mice, n = 3–4; two representative results shown). *P < 0.05; **P < 0.01; ***P < 0.001. C, control; KO, AFHKO.

significantly elevated both under basal conditions and after insulin injection (Fig. 5*G* and Supplementary Fig. 7*C*). These data suggest high insulin sensitivity in AFHKO skeletal muscle.

Despite the leanness of AFHKO mice, their plasma adiponectin level was lower than in controls (Fig. 5*C* and *D*). Adiponectin mRNA levels were similar in AFHKO and control adipose tissues (data not shown). Because succination

of adiponectin in adipocytes can reduce plasma adiponectin level (28), we examined succination in AFHKO adipose tissue. Total adiponectin level was similar in AFHKO mice and controls. In contrast, succinated adiponectin was greatly increased in AFHKO adipose tissue (Supplementary Fig. 8).

AFHKO Mice Are Protected From High-Fat Diet–Induced Obesity, Insulin Resistance, and Hepatic Steatosis

We fed a high-fat diet to AFHKO and control mice starting at 9 weeks of age when their body masses were similar. Thereafter, the mass of controls became progressively greater than that of AFHKO mice (Fig. 6*A*). This difference reached 13.86 g at 5 months ($P < 0.001$) and was explained almost entirely by the lower fat mass of AFHKO mice (12.1 g, $P < 0.001$) (Fig. 6*B*) and reflected histologically and by the masses of individual WAT depots (Supplementary Fig. 9*A* and *B*). In contrast to controls, AFHKO mice remained insulin sensitive and glucose tolerant (Fig. 6*C*), with significantly lower plasma insulin, leptin, TG, NEFA, and adiponectin levels (Fig. 6*D*). After high-fat diet feeding, control but not AFHKO mice developed marked hepatic steatosis (Fig. 6*E–G*).

Food Intake, Energy Expenditure, and Activity Are Normal or High in AFHKO Mice

Food intake, energy expenditure, and activity measured in 5-month-old mice were at least as high in AFHKO as in control animals. AFHKO mice ate more than controls between 9:00 A.M. and 5:00 P.M. and similar amounts during the rest of the day (Supplementary Fig. 10*A*). Fecal weight and fecal lipids (Supplementary Fig. 10*B* and *C*) were similar in AFHKO and control mice. Mean VO_2, CO_2 release, and energy expenditure tended to be higher in AFHKO mice but did not reach significance (Supplementary Fig. 10*D–F*). AFHKO mice were at least as physically active as controls (Supplementary Fig. 10*G*).

At Thermoneutrality, AFHKO Mice Lose Insulin Sensitivity, and Protection From Hepatic Steatosis Is Reduced

Because skeletal muscle–mediated shivering might contribute to the insulin sensitivity of AFHKO mice at room temperature, we tested 9-month-old AFHKO mice that were initially insulin sensitive and glucose tolerant (Fig. 7*A*). After housing these mice for 1 month at thermoneutrality (30°C), insulin sensitivity and glucose tolerance (Fig. 7*B*) became similar to those of controls. Food intake decreased at 30°C in both AFHKO mice and controls (Supplementary Fig. 11*A*). Fat mass remained lower in AFHKO mice than in controls (Supplementary Fig. 11*B*), and the increase of fat mass was less in AFHKO mice (Supplementary Fig. 11*E*). The histological features of AFHKO WAT were preserved, showing small white adipocytes. In BAT, at thermoneutrality, large unilocular brown adipocytes were present as before in AFHKO mice as well as in control mice (Supplementary Fig. 11*C* and *D*).

At 21°C, 10-month-old AFHKO mice were resistant to hepatic steatosis (Fig. 7*C*). Liver mass (Fig. 7*D*) and hepatic TG content (Fig. 7*E*) were significantly lower than in controls. After 1 month at 30°C, the difference in liver fat between AFHKO and normal liver decreased (Fig. 7*C–E*). Mean skeletal muscle TG content at 30°C was slightly higher in both AFHKO and control mice than at 21°C, but this did not reach significance (Supplementary Fig. 11*F*). After 1 month at thermoneutrality, plasma levels of insulin, leptin, NEFA, and adiponectin remained lower in AFHKO mice than in controls (Fig. 7*E–I*). For insulin levels, the difference between AFHKO and control mice was less than at room temperature (Fig. 7*F*).

DISCUSSION

In type 2 diabetes and obesity, mitochondrial function is low in WAT (1–7). AFHKO mice have a primary mitochondrial deficiency in adipose tissue. To our knowledge AFHKO mice are the first strain with isolated adipose deficiency of an enzyme in the mainstream of mitochondrial energy metabolism. AFHKO mice have shown marked ATP depletion and ultrastructural changes similar to those of other mitochondrial diseases (35), including FH-deficient myometria (36) and aP2-TFAM$^{-/-}$ mice (15). Of note, instead of being obese or diabetic, AFHKO mice showed low fat mass, low hepatic fat content, glucose tolerance, and insulin sensitivity despite aging and high-fat diet feeding (Fig. 8).

In WAT, the leanness of AFHKO mice is the opposite result expected from the association of mitochondrial dysfunction and obesity reported in humans and mice (1–7). However, the two conditions are not directly comparable. AFHKO mice have primary complete adipocyte-specific deficiency of one key step of mitochondrial energy metabolism. In contrast, in exogenous obesity and some genetic mitochondrial diseases, a partial multiorgan decrease of mitochondrial function occurs. Considering adipose FH deficiency together with Crif1- and TFAM-deficient mice (14,15,17), in which multiple proteins are affected due to abnormal mitochondrial translation or transcription, a picture emerges that primary adipose-specific mitochondrial deficiency produces leanness. We show that ATP depletion in white adipocytes is strongly associated with reduction of TG synthesis. Chronic imbalance between low TG synthesis and normal lipolysis, both of which were seen in AFHKO mice, is a potential mechanism for the leanness and small WAT adipocyte size of AFHKO mice. The BAT phenotype of AFHKO mice of high BAT mass, cellular enlargement, and monolocular morphology is a frequent finding in many conditions that reduce BAT function (e.g., UCP1, Gsα, TFAM) (17,37,38).

Insulin sensitivity was a robust phenotype of AFHKO mice at room temperature. It was resistant to aging and high-fat diet feeding, and it occurred despite the presence of two features that are normally associated with insulin resistance: inflammation in WAT and low levels of circulating adiponectin. Histologically, the inflammatory

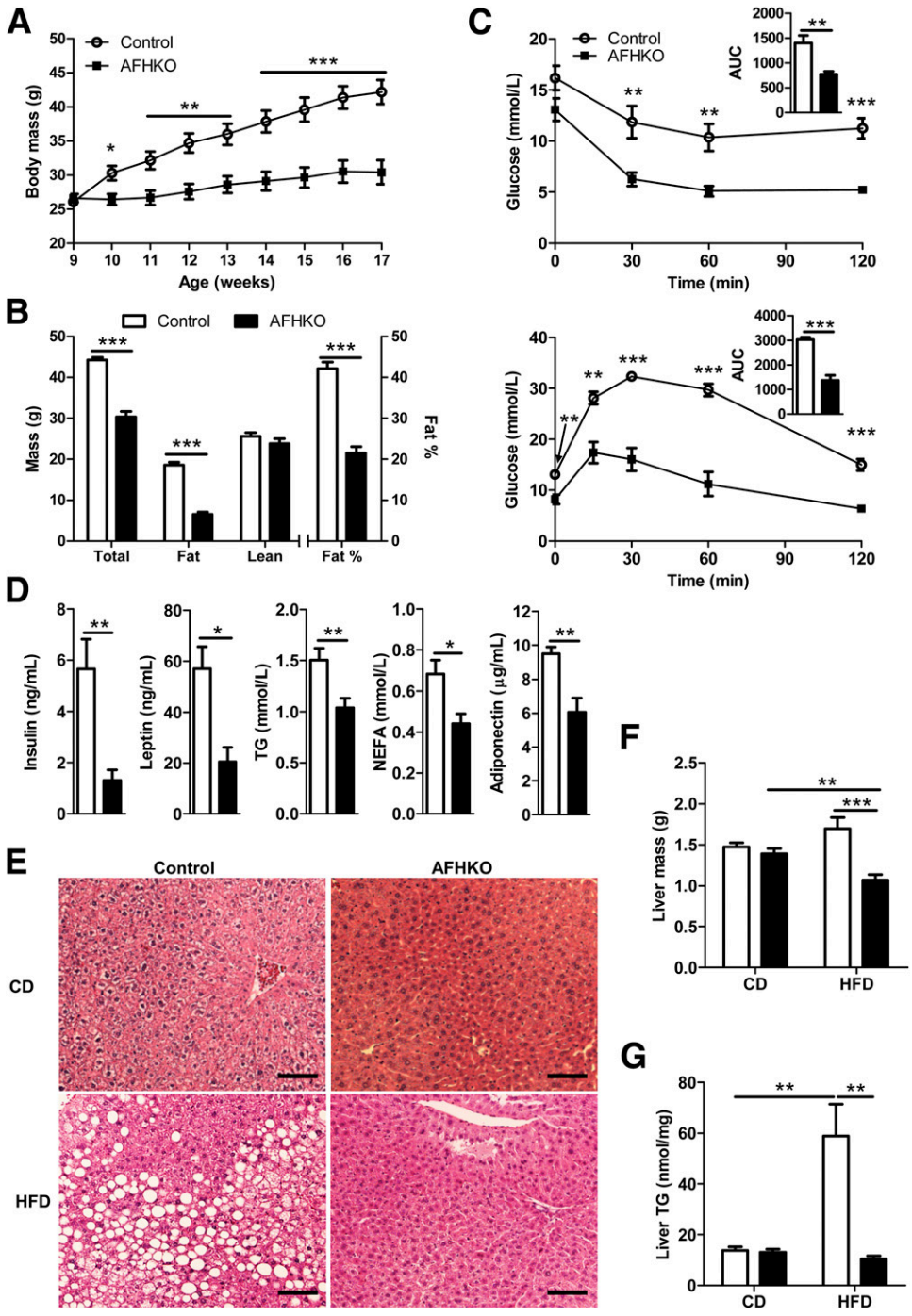

Figure 6—AFHKO mice are resistant to high-fat diet (HFD)–induced obesity and hepatic steatosis, are insulin sensitive, and are glucose tolerant. *A*: Body mass changes on HFD. Control and AFHKO male mice were fed an HFD starting at 9 weeks of age (9 controls, 10 AFHKO). *B*: Body composition (5-month-old mice, $n = 7$). *C*: ITT (top) at 18 weeks of age and GTT (bottom) at 19 weeks of age ($n = 6$). Insets depict areas under the curve (AUCs) in mmol/L · min. *D*: Plasma levels of insulin, leptin, TG, NEFA, and adiponectin ($n = 6$–8). *E*: Representative liver histology of 5-month-old mice on a normal chow diet (CD) or after HFD feeding since 9 weeks of age ($n = 3$). Scale bar = 100 μm. *F* and *G*: Liver mass ($n = 8$) and liver TG content ($n = 6$–8). $^*P < 0.05$; $^{**}P < 0.01$; $^{***}P < 0.001$.

infiltrate in AFHKO adipose tissues was milder than that of Crif1- (14) or TFAM-deficient mice (17). We speculate that in severe mitochondrial disease in adipose tissue, an increased fraction of adipocytes may undergo cell death, stimulating macrophage infiltration as seen in obesity (31). AFHKO mice have low levels of plasma adiponectin, whereas high levels occur in lean mice and humans (39,40). At least two factors may explain this difference. First, high intracellular fumarate can cause increased succination of adiponectin in adipocytes, impairing its multimerization and

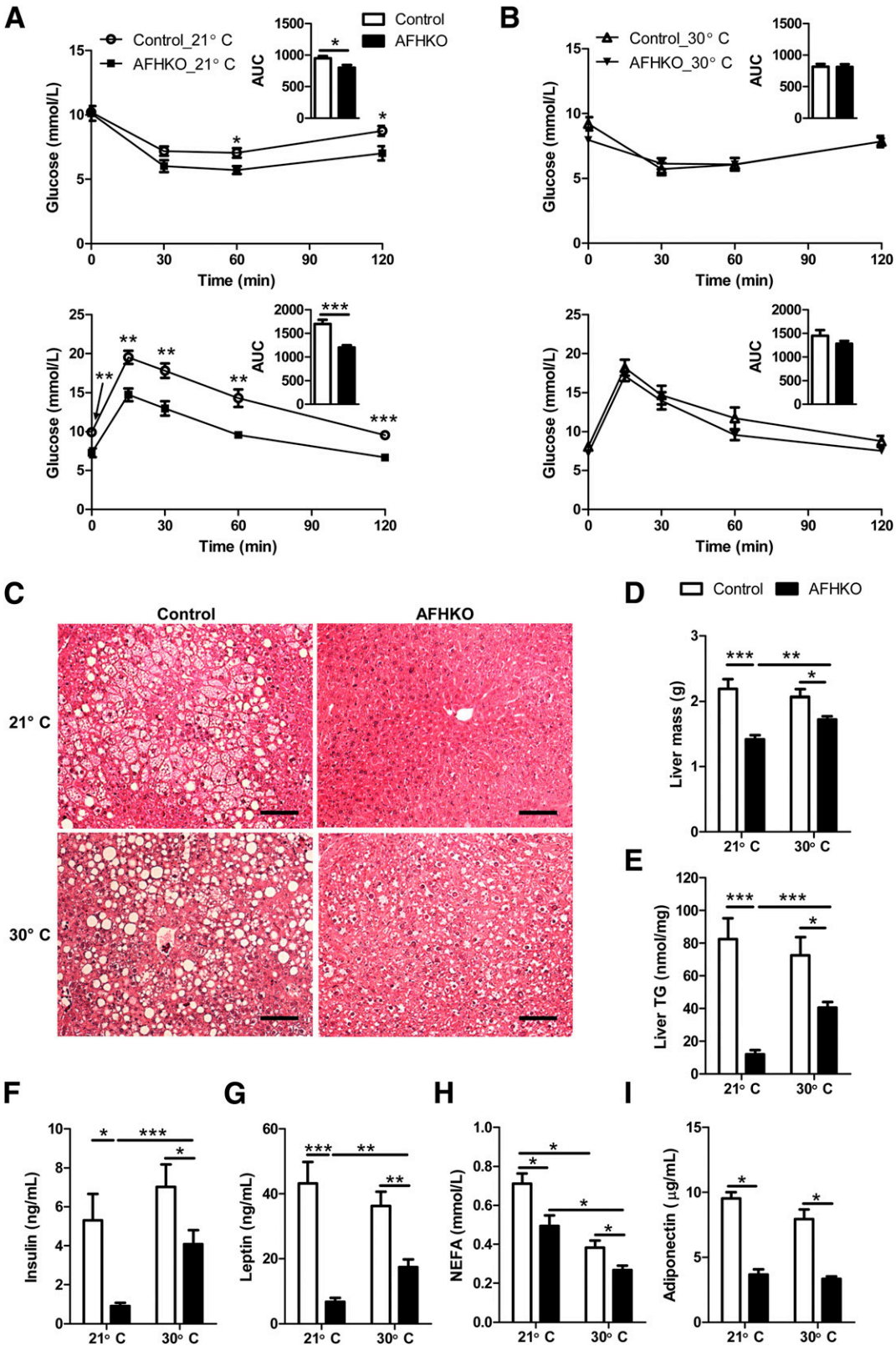

Figure 7—Thermoneutrality reverses insulin sensitivity and reduces resistance to liver steatosis of AFHKO mice. *A*: ITT (top) and GTT (bottom) were performed at 21°C (9-month-old mice, $n = 8$). *B*: ITT (top) and GTT (bottom) of these mice 1 month after transfer to thermoneutrality (30°C). Insets depict areas under the curve (AUCs) in mmol/L · min. *C–E*: Liver histology (three representative sections shown), liver mass ($n = 8$), and liver TG content ($n = 8$), respectively, of 10-month-old mice reared at 21°C and 9-month-old mice reared at 21°C and then housed for 1 month at 30°C. Scale bar = 100 μm. *F–I*: Plasma levels of insulin, leptin, NEFA, and adiponectin before and after 1 month at thermoneutrality (10-month-old mice, $n = 8$). $^{*}P < 0.05$; $^{**}P < 0.01$; $^{***}P < 0.001$.

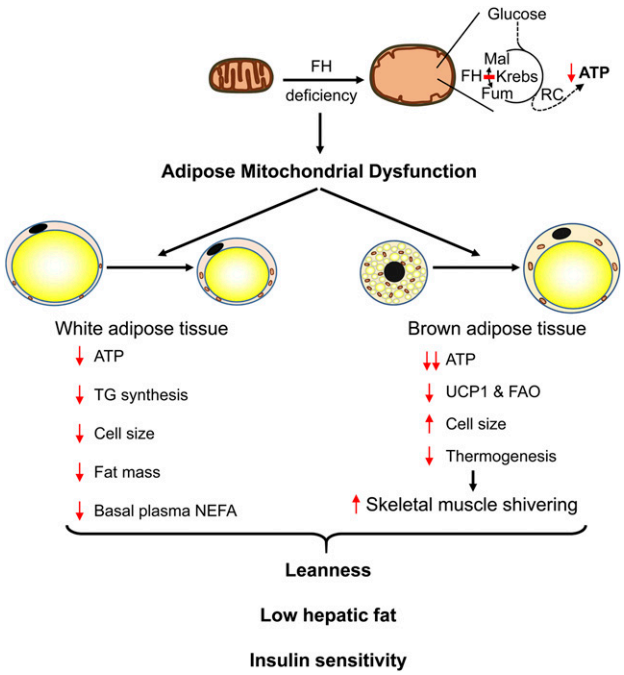

Figure 8—The effects of adipose FH deficiency. FH deficiency disrupts the Krebs cycle and leads to severe mitochondrial dysfunction with altered mitochondrial ultrastructure and low levels of ATP. Adipose FH deficiency in WAT of AFHKO mice causes a reduced capacity for TG synthesis, small cell diameter, low fat mass, and low basal plasma NEFA. In BAT, AFHKO mice show a marked decrease of UCP1 expression, hypertrophic brown adipocytes, and defective thermogenesis. At normal room temperature (21°C), these AFHKO mice are lean and protected against hepatic steatosis and insulin resistance. FAO, fatty acid oxidation; Fum, fumarate; Mal, malate; RC, respiratory chain.

secretion of adiponectin (28). Succination of adiponectin in AFHKO adipose tissue likely contributes to the low level of circulating adiponectin. Second, impaired mitochondrial function and ATP depletion are themselves associated with low adiponectin synthesis (41) and secretion (42,43).

Both WAT and BAT play roles in the insulin sensitivity and low hepatic fat content of AFHKO mice. The low WAT mass and the correspondingly low basal levels of circulating NEFA of AFHKO mice are known protective factors against insulin resistance (44,45). FH deficiency in BAT, however, is the principal factor underlying the insulin sensitivity of AFHKO mice at room temperature. At the typical animal room temperature of 21°C, mice show active thermogenesis (46,47), and these routine housing conditions are considered to be a form of cold stress that can be removed by housing at thermoneutrality. At thermoneutrality, the protective effect of FH deficiency on insulin sensitivity was not detectable, showing the importance of BAT for the insulin sensitivity of AFHKO mice.

The insulin sensitivity of AFHKO mice at room temperature, therefore, can be explained mainly by impaired nonshivering thermogenesis, which will activate skeletal muscle–mediated shivering thermogenesis. Shivering can occur normally in AFHKO mice because their skeletal muscle has normal FH activity. Shivering thermogenesis maintains body temperature and increases energy expenditure, reducing tissue lipid accumulation and protecting from insulin resistance. This is consistent with the severe morphological changes in AFHKO BAT mitochondria, suppression of UCP1 expression, unilocular brown adipocyte morphology, and poor temperature maintenance of AFHKO mice. Also consistent with this mechanism, mean values for VO_2 and energy expenditure were persistently slightly greater in AFHKO mice than in controls at room temperature, although this was not statistically significant. As discussed for other models (48,49), chronic small changes below current limits of resolution may contribute importantly to energy homeostasis and body weight. In conclusion, AFHKO mice are similar to other models of BAT dysfunction, such as UCP1- and Gsα-deficient mice (38,47), in which low UCP1 expression and increased shivering thermogenesis are well documented.

Mitochondrial dysfunction in adipose tissue has been studied mainly in mitochondrial diseases, obesity, and diabetes (1–7). In these conditions, adipose tissue mitochondrial deficiency is only one element of a complex metabolic network. Models of adipose-specific mitochondrial deficiency may be useful for studying genes like FH that are lethal if deficient in all tissues (25). AFHKO mice reveal that adipose tissue mitochondria are important for the normal function of adipose tissue and for systemic physiology. They show that in some situations, adipose mitochondrial deficiency can protect against the development of obesity and diabetes.

Funding. This work was supported in part by Canadian Institutes for Health research grant 221920 to G.A.M.

Duality of Interest. No potential conflicts of interest relevant to this article were reported.

Author Contributions. H.Y. contributed to the study concept and design, experiments, data analysis, and writing and critical review of the manuscript. J.W.W. and S.P.W. contributed to the experiments, data analysis, and critical review of the manuscript. I.S., L.S., and S.C. contributed to the transmission electron microscopy, data analysis, and critical review of the manuscript. N.F. contributed to the detection of protein succination, data analysis, and critical review of the manuscript. G.Y. contributed to the study design, discussion, and critical review of the manuscript. G.A.M. contributed to the study concept and design and writing and critical review of the manuscript. G.A.M. is the guarantor of this work and, as such, had full access to all the data in the study and takes responsibility for the integrity of the data and the accuracy of the data analysis.

References

1. Yin X, Lanza IR, Swain JM, Sarr MG, Nair KS, Jensen MD. Adipocyte mitochondrial function is reduced in human obesity independent of fat cell size. J Clin Endocrinol Metab 2014;99:E209–E216

2. Heinonen S, Buzkova J, Muniandy M, et al. Impaired mitochondrial biogenesis in adipose tissue in acquired obesity. Diabetes 2015;64:3135–3145

3. Patti ME, Corvera S. The role of mitochondria in the pathogenesis of type 2 diabetes. Endocr Rev 2010;31:364–395

4. Pietiläinen KH, Naukkarinen J, Rissanen A, et al. Global transcript profiles of fat in monozygotic twins discordant for BMI: pathways behind acquired obesity. PLoS Med 2008;5:e51

5. Dahlman I, Forsgren M, Sjögren A, et al. Downregulation of electron transport chain genes in visceral adipose tissue in type 2 diabetes independent of obesity and possibly involving tumor necrosis factor-alpha. Diabetes 2006;55: 1792–1799
6. Choo HJ, Kim JH, Kwon OB, et al. Mitochondria are impaired in the adipocytes of type 2 diabetic mice. Diabetologia 2006;49:784–791
7. Rong JX, Qiu Y, Hansen MK, et al. Adipose mitochondrial biogenesis is suppressed in db/db and high-fat diet-fed mice and improved by rosiglitazone. Diabetes 2007;56:1751–1760
8. Cannon B, Nedergaard J. Studies of thermogenesis and mitochondrial function in adipose tissues. Methods Mol Biol 2008;456:109–121
9. Kusminski CM, Scherer PE. Mitochondrial dysfunction in white adipose tissue. Trends Endocrinol Metab 2012;23:435–443
10. Fedorenko A, Lishko PV, Kirichok Y. Mechanism of fatty-acid-dependent UCP1 uncoupling in brown fat mitochondria. Cell 2012;151:400–413
11. Harms M, Seale P. Brown and beige fat: development, function and therapeutic potential. Nat Med 2013;19:1252–1263
12. Fu Y, Luo N, Lopes-Virella MF. Oxidized LDL induces the expression of ALBP/aP2 mRNA and protein in human THP-1 macrophages. J Lipid Res 2000;41:2017–2023
13. Elmasri H, Karaaslan C, Teper Y, et al. Fatty acid binding protein 4 is a target of VEGF and a regulator of cell proliferation in endothelial cells. FASEB J 2009;23:3865–3873
14. Ryu MJ, Kim SJ, Kim YK, et al. Crif1 deficiency reduces adipose OXPHOS capacity and triggers inflammation and insulin resistance in mice. PLoS Genet 2013;9:e1003356
15. Vernochet C, Mourier A, Bezy O, et al. Adipose-specific deletion of TFAM increases mitochondrial oxidation and protects mice against obesity and insulin resistance. Cell Metab 2012;16:765–776
16. Lee KY, Russell SJ, Ussar S, et al. Lessons on conditional gene targeting in mouse adipose tissue. Diabetes 2013;62:864–874
17. Vernochet C, Damilano F, Mourier A, et al. Adipose tissue mitochondrial dysfunction triggers a lipodystrophic syndrome with insulin resistance, hepatosteatosis, and cardiovascular complications. FASEB J 2014;28:4408–4419
18. Suzuki T, Yoshida T, Tuboi S. Evidence that rat liver mitochondrial and cytosolic fumarases are synthesized from one species of mRNA by alternative translational initiation at two in-phase AUG codons. Eur J Biochem 1992;207:767–772
19. Ratner S, Anslow WP Jr, Petrack B. Biosynthesis of urea. VI. Enzymatic cleavage of argininosuccinic acid to arginine and fumaric acid. J Biol Chem 1953; 204:115–125
20. Cohen PP, Hayano M. The conversion of citrulline to arginine (transimination) by tissue slices and homogenates. J Biol Chem 1946;166:239–250
21. Allegri G, Fernandes MJ, Scalco FB, et al. Fumaric aciduria: an overview and the first Brazilian case report. J Inherit Metab Dis 2010;33:411–419
22. Rustin P, Bourgeron T, Parfait B, Chretien D, Munnich A, Rötig A. Inborn errors of the Krebs cycle: a group of unusual mitochondrial diseases in human. Biochim Biophys Acta 1997;1361:185–197
23. Stewart L, Glenn GM, Stratton P, et al. Association of germline mutations in the fumarate hydratase gene and uterine fibroids in women with hereditary leiomyomatosis and renal cell cancer. Arch Dermatol 2008;144:1584–1592
24. Pithukpakorn M, Toro JR. Hereditary leiomyomatosis and renal cell cancer. In *GeneReviews*®. Pagon RA, Adam MP, Ardinger HH, et al., Eds. Seattle, WA, University of Washington, 1993
25. Pollard PJ, Spencer-Dene B, Shukla D, et al. Targeted inactivation of fh1 causes proliferative renal cyst development and activation of the hypoxia pathway. Cancer Cell 2007;11:311–319
26. Sirois J, Côté JF, Charest A, et al. Essential function of PTP-PEST during mouse embryonic vascularization, mesenchyme formation, neurogenesis and early liver development. Mech Dev 2006;123:869–880
27. Wu JW, Wang SP, Casavant S, Moreau A, Yang GS, Mitchell GA. Fasting energy homeostasis in mice with adipose deficiency of desnutrin/adipose triglyceride lipase. Endocrinology 2012;153:2198–2207
28. Frizzell N, Rajesh M, Jepson MJ, et al. Succination of thiol groups in adipose tissue proteins in diabetes: succination inhibits polymerization and secretion of adiponectin. J Biol Chem 2009;284:25772–25781
29. Danson MJ, Hough DW. Citrate synthase from hyperthermophilic archaea. Methods Enzymol 2001;331:3–12
30. Bardella C, Olivero M, Lorenzato A, et al. Cells lacking the fumarase tumor suppressor are protected from apoptosis through a hypoxia-inducible factor-independent, AMPK-dependent mechanism. Mol Cell Biol 2012;32:3081–3094
31. Cinti S, Mitchell G, Barbatelli G, et al. Adipocyte death defines macrophage localization and function in adipose tissue of obese mice and humans. J Lipid Res 2005;46:2347–2355
32. Fortier M, Wang SP, Mauriège P, et al. Hormone-sensitive lipase-independent adipocyte lipolysis during beta-adrenergic stimulation, fasting, and dietary fat loading. Am J Physiol Endocrinol Metab 2004;287:E282–E288
33. Sillerud LO, Han CH, Bitensky MW, Francendese AA. Metabolism and structure of triacylglycerols in rat epididymal fat pad adipocytes determined by ^{13}C nuclear magnetic resonance. J Biol Chem 1986;261:4380–4388
34. Kraus D, Yang Q, Kahn BB. Lipid extraction from mouse feces. Bio Protoc 2015;5:5
35. DiMauro S, Hirano M, Schon EA. *Mitochondrial Medicine*. Abingdon, U.K., Informa Healthcare, 2006
36. Wortham NC, Alam NA, Barclay E, et al. Aberrant expression of apoptosis proteins and ultrastructural aberrations in uterine leiomyomas from patients with hereditary leiomyomatosis and renal cell carcinoma. Fertil Steril 2006;86:961–971
37. Enerbäck S, Jacobsson A, Simpson EM, et al. Mice lacking mitochondrial uncoupling protein are cold-sensitive but not obese. Nature 1997;387:90–94
38. Chen M, Chen H, Nguyen A, et al. G(s)alpha deficiency in adipose tissue leads to a lean phenotype with divergent effects on cold tolerance and diet-induced thermogenesis. Cell Metab 2010;11:320–330
39. Yamauchi T, Kamon J, Waki H, et al. The fat-derived hormone adiponectin reverses insulin resistance associated with both lipoatrophy and obesity. Nat Med 2001;7:941–946
40. Arita Y, Kihara S, Ouchi N, et al. Paradoxical decrease of an adipose-specific protein, adiponectin, in obesity. Biochem Biophys Res Commun 1999;257:79–83
41. Koh EH, Park JY, Park HS, et al. Essential role of mitochondrial function in adiponectin synthesis in adipocytes. Diabetes 2007;56:2973–2981
42. Wang CH, Wang CC, Huang HC, Wei YH. Mitochondrial dysfunction leads to impairment of insulin sensitivity and adiponectin secretion in adipocytes. FEBS J 2013;280:1039–1050
43. Szkudelski T, Nogowski L, Szkudelska K. Short-term regulation of adiponectin secretion in rat adipocytes. Physiol Res 2011;60:521–530
44. Boden G. Obesity, insulin resistance and free fatty acids. Curr Opin Endocrinol Diabetes Obes 2011;18:139–143
45. den Boer M, Voshol PJ, Kuipers F, Havekes LM, Romijn JA. Hepatic steatosis: a mediator of the metabolic syndrome. Lessons from animal models. Arterioscler Thromb Vasc Biol 2004;24:644–649
46. Karp CL. Unstressing intemperate models: how cold stress undermines mouse modeling. J Exp Med 2012;209:1069–1074
47. Feldmann HM, Golozoubova V, Cannon B, Nedergaard J. UCP1 ablation induces obesity and abolishes diet-induced thermogenesis in mice exempt from thermal stress by living at thermoneutrality. Cell Metab 2009;9:203–209
48. Butler AA, Kozak LP. A recurring problem with the analysis of energy expenditure in genetic models expressing lean and obese phenotypes. Diabetes 2010;59:323–329
49. Tseng YH, Cypess AM, Kahn CR. Cellular bioenergetics as a target for obesity therapy. Nat Rev Drug Discov 2010;9:465–482